African Scientist Vol. 24, No. 2 June 30, 2023
Printed in Nigeria

1595-6881/2023 $80.00 + 0.00

https://africanscientistjournal.org

AFS2023025/24209

Discovery of Eriodictyol as Putative Exportin-1 Inhibitor for Non-small Cell Lung Cancer Therapy

Temidayo Olamide Adigun[1*], Faoziyat Adenike Sulaiman[1], Asiat Na'Allah[5], Mutiu A. Alabi[5], Christian Emeka Odo[6], Eunice Toluwalope Adebamiji[1], Itunu Ayomikun Oluwadare[1], Ugochukwu Okechukwu Ozojiofor[2], Adedayo Pius Omoniyi[3], Wisdom O. Joel[7], Kehinde Oyebola Aina[1], Omokolade O. Alejolowo[4], Saheed Olatunbosun Akiode[8], Janet F. Adeegbe[9]

[1]Department of Biochemistry, Faculty of Life Sciences, University of Ilorin, Ilorin, Nigeria
[2]Department of Biotechnology, Nigeria Defence Academy, Kaduna, Nigeria
[3]Department of Biochemistry, School of Science, Federal University of Technology Akure, Akure, Nigeria
[4]Department of Biochemistry, Landmark University, Omu-Aran
[5]Department of Biochemistry, Faculty of Pure and Applied Sciences, Kwara State University, Malete
[6]Department of Biochemistry, College of Natural Sciences, Michael Okpara University of Agriculture, Umudike
[7]Department of Biochemistry, College of Science and Technology, Covenant University, Ota, Nigeria
[8]Biotechnology Advanced Research Centre, Sheda Science and Technology Complex (SHESTCO), P.M.B. 186, Garki, Abuja, Nigeria
[9]Bioresources Development Centre, National Biotechnology Development Agency, Ogbomoso, Nigeria.

*Corresponding author Email: prothesis4life@gmail.com Tel: +234 (0) 816 644 8182

(Received May 25, 2023; Accepted in revised form May 31, 2023)

ABSTRACT: Exportin-1, the ubiquitous nuclear protein transporter, is widely confirmed as an active chemotherapeutic target in non-small cell lung cancer conditions, while *Juglans mandshurica* is a well-studied anticancer plant in some lung cancer cell lines. We intend to find a novel exportin-1 inhibitor from *Juglans mandshurica* with better potential, tolerability and pharmaco-dynamo-kinetic properties than the current selective inhibitors of nuclear export in non-small cell lung cancer treatment. OSIRIS DataWarrior, along with Glide standard precision docking, and other Glide modules were employed for compound properties exploration, docking simulations, free energy calculations against exportin-1; density functional theory analysis of the compounds were carried out to estimate their electronic stability, while web-based SWISSADME was employed for ADMET and synthetic accessibility evaluations. This study reveals eriodictyol as having higher binding free energy (-40 kcal/mol) than that of standard (-39.56 kcal/mol) in exportin-1 active site, better synthetic accessibility score (3.15 versus 3.29), high GI absorption, non-blood brain barrier permeant, lacks Brenk and PAINS alert, obeying Lipinski's, Ghose's, Veber's, Egan's, and Muegge's rule of drug-likeness and lead-likeness as well as non-cytotoxic to HepG2 cells. We therefore found eriodictyol as a lead-like, non-toxic exportin-1 inhibitor with good predictive stability and pharmacokinetic potential and thus provided data for further validation of eriodictyol as a candidate exportin-1 inhibitor in both preclinical and clinical studies involving lung cancer therapy.

Keywords: Exportin-1, Eriodictyol, *Juglans mandshurica*, Non-small cell lung cancer

Introduction

Exportin-1 (XPO-1), also known as chromosomal region maintenance 1 (CRM 1), is an essentially active ubiquitous exporter of more than 1050 protein cargoes from the human cell nucleus to cytoplasm according to recent deep proteomic characterization studies of nucleocytoplasmic organization of eukaryotic cells (Kirli *et al*., 2015; Zhu *et al*., 2019). It recognizes leucine-rich signals on intranuclear cargo proteins containing tumour

suppressor proteins (such as p53, p73, p21, p27 etc.) and other cell cycle regulators (such as retinoblastoma, adenomatous polyposis coli, forkhead box O, activator of transcription 3, inhibitor of kappa B-alpha, protease-activated receptor 4, topoisomerase II, galectin-3 etc.) and mediates their RanGTP-driven transport into the cytoplasm (Sun *et al*., 2014; Sun *et al*., 2016).

Exportin-1 carries out this active process in a regulatory way under normal physiological conditions but becomes dysregulated, via overexpression, in cancer conditions (Wang and Liu, 2019). This drives oncogenic features such as aberrant growth signaling, apoptosis inactivation, angiogenesis sustenance as well as its association with drug resistance (due to excessively dislocated drug targets such as topoisomerase II, galectin-3 etc.) in non-small cell lung cancer (NSCLC), including the highly untreatable KRAS-mutant lung adenocarcinoma (Sun *et al*., 2014).

Exportin-1 is frequently amplified and/or mutated (e.g., the clinically relevant gain-of-function mutation such as E571K and R749Q) with its over-expression correlating with poor prognosis in NSCLC patients (Gupta *et al*., 2017; Zhu *et al*., 2019). Targeting XPO1 alone by the recently developed selective inhibitors of nuclear export (SINE) (e.g., the widely studied KPT-330 (Selinexor), KPT-185, KPT-225, KPT-276 etc.) or in combination with other targeted therapies or chemotherapies have shown broad anticancer effect and acceptable tolerance (Zhu *et al*., 2019).

Although several orally bioavailable inhibitors of XPO1 have been developed, with many of them currently showing promising efficacy whether as a single anticancer agent or synergistically in combination regimens under clinical trials (Gupta *et al*., 2017; Azizian and Li, 2020), their effects remain limited by their low safety profiles, including the brain-associated adverse effects like anorexia, weight loss etc., as well as haematologic adverse effects such as thrombocytopaenia (Zhu *et al*., 2019; Azizian and Li, 2020). These have been associated respectively with the blood brain barrier penetrability and the off-target effects of some of these inhibitors, with reduced tolerability in cancer patients (Azizian and Li, 2020). Also, KPT-185 has been shown to possess unsuitable pharmacokinetic properties *in vivo*, either subcutaneously or orally, in a pre-clinical study (Zhang *et al*., 2013).

We aim to find out in this study whether there is a better potential selective inhibitor (s) of nuclear export (SINE) among the various compounds identified and isolated from *Juglans mandshurica* in some reports (Guo *et al*., 2015; Jahaban-Esfahlan *et al*., 2019; Luo *et al*., 2017). Also, we aim to determine whether these potential inhibitor (s) may have better predictive tolerability and suitable pharmacokinetic properties than the currently known SINE compounds for treating non-small cell lung cancer condition.

Several drug entities from nature (the master craftsman of molecules) have been used to cure various ailments since the inception of first known human civilization while plants remain an infinite resource harbouring promising novel chemotypic drug development against cancer (Veeresham, 2012; Wannes *et al*., 2018). Indeed, several current standard-of-care drugs (with relatively few side effects) are known to have been developed from plants such as the alkaloids vinblastine (from *Catharanthus roseus*), paclitaxel (from *Taxus brevifolia*) while more phytochemicals are showing great promises for cancer prevention and treatment in many preclinical and clinical studies (Zhang *et al*., 2015; Asadi-Samani *et al*., 2016; Wannes *et al*., 2018).

Materials and methods

Softwares and tools employed: National Center of Biotechnology Institute (NCBI), Research Collaboratory Structural Bioinformatics Protein Database (RCSB PDB), NCBI PubChem Database, Schrödinger PyMol®, Schrödinger Maestro Glide, Schrödinger Quantum Polarized Ligand Docking module, Schrödinger Maestro Prime, Schrödinger Maestro Prime, Schrödinger Maestro Jaguar, PyRx AutoDock Vina, Molegro Virtual Docking Program, Argus Lab, online web-based SwissDock (http://www.swissdock.ch/index.ph), Biovia Discovery Studio suite, online web-based SwissADME (http://www.swissadme.ch/index.ph), ChemAxon Marvin Sketch.

Target preparation: The PDB coordinate files (PDB ID: 3GB8) of human (*Homo sapiens*) crystal structure of chromosomal region maintenance 1 (CRM 1)-Snurportin-1 complex was retrieved from the protein data bank (http://www.rcsb.org), visualized using the Schrodinger molecular graphics program PyMol® and prepared using Schrodinger maestro protein preparation wizard. Briefly, the Snuportin-l chain (chain B) was deleted from the complex while the remainder (chain A) was prepared under OPLS2005 force field at pH 7.0±2.0. All stearic clashes were corrected, hydrogen bond order fixed while the missing side chains and loops were corrected using prime. Disulfide bonds were created, water molecules beyond 5.00Å were removed from the ionized (Het) groups, water molecules (co-crystallized with target) with less than 3 hydrogen bonds to non-waters were deleted while the bond orders were assigned. The charge cutoff for polarity was 0.25.

Ligand preparation: We retrieved the two-dimensional structures of compounds identified and isolated from various parts and extracts of *Juglans mandshurica* in some studies (Guo *et al*., 2015; Luo *et al*., 2017; Jahaban-Esfahlan *et al*., 2019) while the structures of compounds (Compound A, B, C, D, E, F, Y, Z) unavailable in PubChem database were designed using ChemAxon Marvin sketch. All the compounds were converted into 3D SDF format before being filtered based on Lipinsky's rule, total polar surface area (TPSA) ≤ 140Å as well as number of rotatable bonds ≤ 10, using DataWarrior v 5.2.1 to retain those that meet these criteria. These were, in addition, pre-filtered based on their tumorigenicity, mutagenicity, irritant properties, nasty functions, drug-likeness, molecular flexibility and complexity. The ligands were prepared using Schrodinger Maestro ligand preparation wizard. Briefly, the ligands were desalted, possible epik states and tautomers were generated at the target pH of 7.0±2.0, specified chirality were retained while other chiral centers were varied.
Ligand docking: Sampled flexible ligand (based on nitrogen inversion and ring conformations) were docked into target sitemap-generated receptor grid using Glide standard precision docking procedure and post docking minimization were performed. Input partial charges were used in calculating the docking score while the ligand with more than 500 atoms was excluded from docking nor scored. The van der Waals radii of ligand atoms with partial atomic charge were scaled with factor of 0.80 less than the partial charge cut-off of 0.15 and the Epik state penalties were added to the docking score.
Quantum mechanics polarized ligand docking: The ligand charges for the initial Glide docking were generated using the standard semi-empirical method precision in which the pose was discarded as duplicate if both root mean square deviation is less than 0.5Å and the maximum atomic displacement is less than 1.3Å. The quantum mechanics charges were calculated for free ligands in the gas phase using the Coulson charge semi-empirical method before redocking at standard precision. Ligands, with their best binding pose, were finally selected based on the Glide Score while the van der Waals scaling was at 1.0 and 0.8 respectively for the receptor and ligand.
Validation of docking study: The docking protocol of this study was validated by redocking of the same standard compound into the same target binding site and examining the relative binding pose of the ligands using the Python Molecular Viewer (PyMol®) graphics software while the docking scores was validated by docking both the lead and standard compound with different docking algorithms including Molegro virtual docking program (based on re-rank score calculated from both MolDock and PLANTS scoring function), Argus Lab (based on AScore scoring function at the best ligand pose), PyRx Autodock Vina (based on Vina scoring function) as well as the online web-based SwissDock (based on evolutionary algorithm docking scoring function).
Binding free energy calculation: Prime was used to calculate the molecular mechanics generalized Born surface area free energy change (MMGBSA dG) of the docked ligands by considering the input ligand partial charges on the VSGB solvation model. Constraints were applied on the flexible residues and their distances were defined using all processed ligands.
Target-ligand interaction representation: The docked ligands in complex with the targets and their respective binding poses were generated using Glide merging procedure while the two-dimensional interactions between the ligands and the target binding pocket residues were visualized using BIOVIA discovery studio suite and PyMol® respectively.
Density functional theory analysis: The molecular orbital energy (represented by HOMO, LUMO, and gap energy), atomic electrostatic potential energy (ESP), and vibrational frequencies of the compounds were calculated by using Jaguar single point energy estimator in water solvation model (having dielectric constant of 80.37).
In-silico pharmacokinetics and toxicity properties profiling: The resultant lead compounds from this study were profiled for their absorption, distribution, metabolism, excretion, and toxicity properties by using the online web-based predictive tool SwissADME (http://www.swissadme.ch/index.php).
Study workflow: The workflow of the various modelling and simulations carried out in this study is as shown in Figure 1.

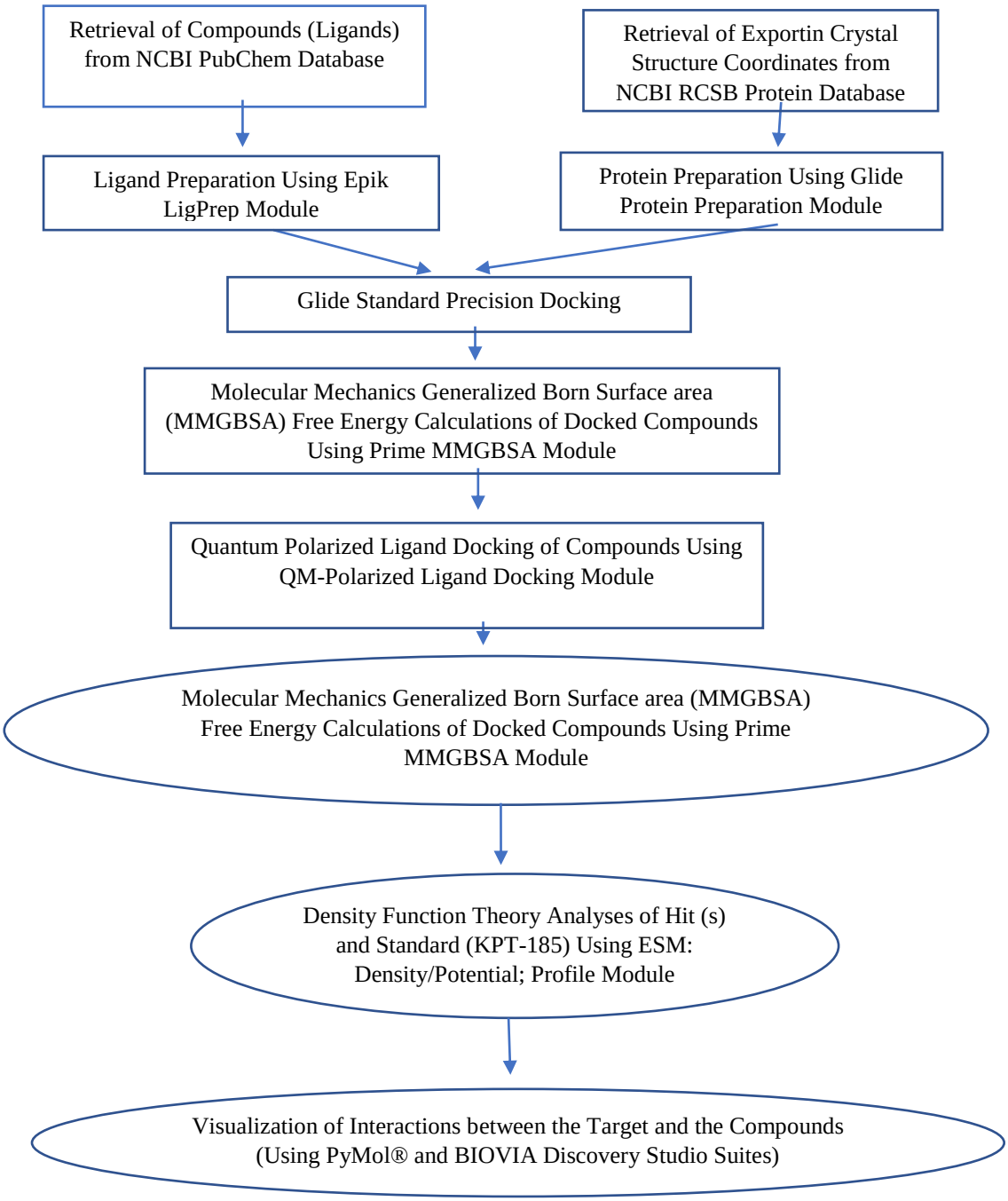

Figure 1: Workflow of step-by-step processes and methods carried out in the study

Results

Compounds retrieved: The total of 133 compounds reported by some studies (Guo *et al*., 2015; Luo *et al*., 2017; Jahaban-Esfahlan *et al*., 2019) were retrieved in this study while a total of 22 (Table 1) with predictably non-toxic and drug-like compounds were recovered following the pre-filtering workflow on Osiris property explorer. Compound A-F, Y, Z were the identified but non-designated compounds from *Juglans mandshurica* with currently no structural information in the PubChem database while the first-generation SINE compound KPT-185 (PubChem CID: 53495165) was evaluated as the standard compound.

Table 1: The retrieved compounds and their simplified molecular input line entry system representation following drug-likeness and toxicity filters

Compound	Canonical SMILES
3-Methoxyjuglone	O=C1c2c(O)cccc2C(=O)C=C1OC
O-Methyljuglone	O=C1c2c(OC)cccc2C(=O)C=C1
Compound A	O=C1c2c(O)cccc2C(=O)C2=C1C1(O)c3c(C(=O)[C@@H]2C1)c(O)ccc3
Isosclerone	O=C1c2c(O)cccc2[C@H](CC1)O
Sclerone	O=C1c2c(c(O)ccc2)[C@H](CC1)O
Compound B	O=C1c2c(O)cccc2C2(CC1C(c1c2cc(c(c1)O)O)CC(=O)O)O
Compound C	Br.Oc1c(cccc1)C12C(N(C(C2)CCC1)C)C
Caffeic acid	O=C(O)/C=C/c1cc(O)c(cc1)O
Ferulic acid	O=C(O)/C=C/c1cc(OC)c(cc1)O
P-Coumaric acid	O=C(O)/C=C/c1ccc(cc1)O
Sinapic acid	O=C(O)/C=C/c1cc(OC)c(c(c1)OC)O
L-Epicatechin	O1c2c(c(O)cc(c2)O)CC(C1c1cc(O)c(cc1)O)O
Eriodictyol	O=C1c2c(O[C@@H](C1)c1cc(O)c(cc1)O)cc(cc2O)O
Epidihydrophaseic acid	O=C(O)/C=C(/C=C/C1(O)C2(OCC1(CC(C2)O)C)C)\C
L-Ascorbic acid	O=C1O[C@@H](C(=C1O)O)C(O)CO
1(2H)-Naphthalenone	O=C1c2c(cccc2)[C@H](CC1)O
(4S)-4alpha Methoxy-S Hydroxytetralin-1-one	O=C1c2c(c(O)ccc2)[C@H](CC1)OC
Compound D	O=C1c2c(c(O)ccc2)[C@H](CC1)O.Oc1ccccc1
Compound E	O=C1c2c(O)ccc(c2[C@H](CC1)OC)O.Oc1ccccc1
Compound F	O=C1c2c(c(O)ccc2)[C@H](CC1)OC.Oc1ccccc1
Compound Y	O=C1c2c(O)cccc2C(CC1)OC1c2c(O)cccc2C(=O)CC1
Compound Z	O=C1c2c(O)cccc2C(CC1)OC1/C(=C/O)/C(=C/O)/C(=O)CC1

Physicochemical properties of retrieved compounds: The 22 compounds retrieved in this study have molecular weights ranging from 162.19 to 356.33, calculated water: octanol partition coefficient (ClogP) ranging from -3.1715 to 2.4646, hydrogen bond acceptors ranging from 2-7, hydrogen bond donors ranging from 0-5, rotatable bond counts ranging from 0-4, as well as total polar surface area ranging from 23.47-135.29 as shown in Table 2.

Table 2: Physicochemical properties of retrieved compounds

Molecule Name	Molecular Weight	ClogP	H-bond Acceptors	H-bond Donors	Polar Surface Area (Å)	Rotatable Bonds
3-Methoxyjuglone	204.181	1.0218	4	1	63.6	1
O-Methyljuglone	188.182	1.3694	3	0	43.37	1
Compound A	348.309	1.8755	6	3	111.9	0
Isosclerone	178.186	1.1939	3	2	57.53	0
Sclerone	178.186	1.1939	3	2	57.53	0
Compound B	356.329	1.6467	7	5	135.29	2
Compound C	312.25	2.5243	2	1	23.47	1
Caffeic acid	180.159	0.7825	4	3	77.76	2
Ferulic acid	194.185	1.0582	4	2	66.76	3
P-Coumaric acid	164.16	1.1282	3	2	57.53	2
Sinapic acid	224.211	0.9882	5	2	75.99	4
L-Epicatechin	290.27	1.5087	6	5	110.38	1
Eriodictyol	288.254	1.81	6	4	107.22	1
Epidihydrophaseic acid	282.335	1.0554	5	3	86.99	3
L-Ascorbic acid	176.124	- 2.4646	6	4	107.22	2
1(2H)- Naphthalenone	162.187	1.5396	2	1	37.3	0
(4S)-4alpha Methoxy-S Hydroxytetralin-1-one	192.213	1.6218	3	1	46.53	1
Compound D	272.299	1.1939	3	2	57.53	0
Compound E	302.325	1.2761	4	2	66.76	1
Compound F	286.326	1.6218	3	1	46.53	1
Compound Y	338.358	3.1715	5	2	83.83	2
Compound Z	330.335	0.9801	6	3	104.06	2

Toxicity profile and drug-likeness of retrieved compounds: The pre-filtered 22 compounds showed predictive toxicity level of none (no risk) to low (low risk) for tumorigenicity, mutagenicity, teratogenicity and irritant properties with quantitative estimate of drug-likeness (QED) range of -1.3232 to 1.9964 as shown in Table 3.

Table 3: Toxicity profile and drug-likeness score of retrieved compound

Molecule Name	Mutagenic	Tumorigenic	Reproductive Effectiveness	Irritant	QED
3-Methoxyjuglone	None	None	None	None	0.6467
O-Methyljuglone	None	None	None	None	0.3379
Compound A	None	None	None	None	1.3461
Isosclerone	None	None	None	None	-1.0249
Sclerone	None	None	Low	None	-1.0249
Compound B	None	None	None	None	0.7503
Compound C	None	None	None	None	1.2862
Caffeic acid	None	None	None	None	0.1675
Ferulic acid	None	None	None	None	0.2751
P-Coumaric acid	None	None	None	None	0.1675
Sinapic acid	None	None	None	None	0.2751
L-Epicatechin	None	None	None	None	0.3153
Eriodictyol	None	None	None	None	-0.2201
Epidihydrophaseic acid	None	None	None	None	1.9964
L-Ascorbic acid	None	None	None	None	0.0238
1(2H)-Naphthalenone	None	None	None	None	-1.0249
(4S)-4alpha Methoxy-S Hydroxytetralin-1-one	None	None	None	None	-1.1964
Compound D	None	None	None	None	-1.0249
Compound E	None	None	None	None	-1.1964
Compound F	None	None	None	None	-1.1964
Compound Y	None	None	None	None	-1.3232
Compound Z	None	None	None	None	-0.2905

Conformational flexibility and complexity scores of retrieved compounds: The molecular complexity scores (shown in Figure 2) of the 22 retrieved compounds in this study are in the range of 0.50742 to 1.0424 on the scale of 0.1 – 1.5, while the molecular flexibility scores (shown Figure 1) of the compounds are in the range of 0.08271 to 0.50646 on a scale of 0.0 (flexible) to 1.0 (completely rigid).

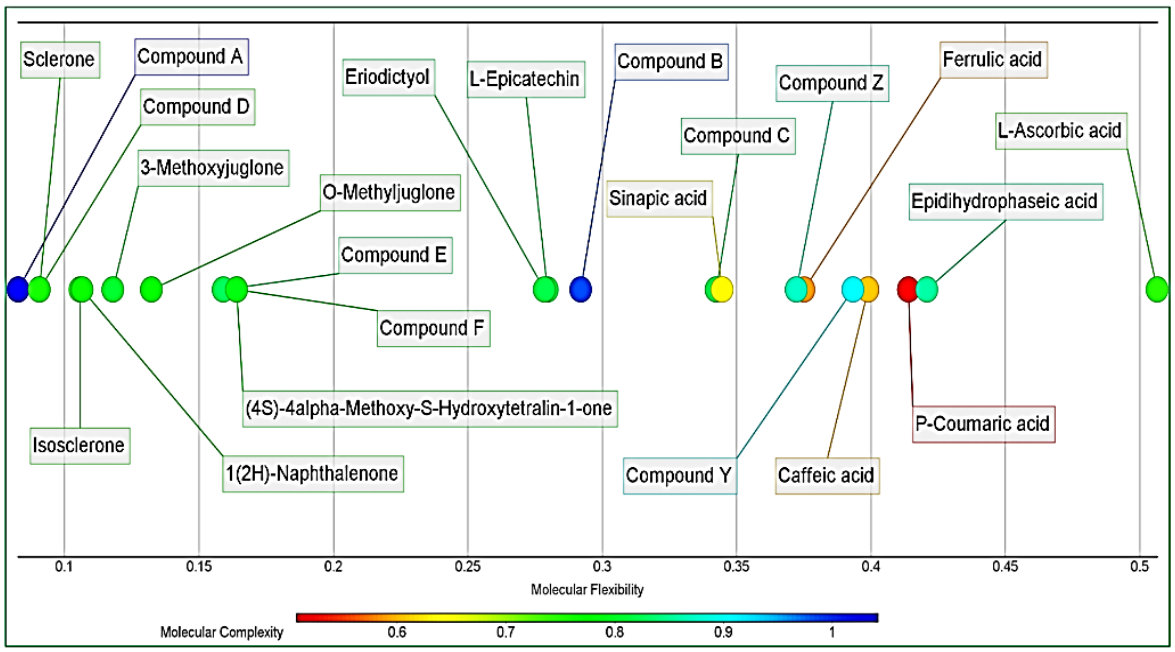

Figure 2: Flexibility and complexity scores of retrieved compounds

Site-specific ligand docking results: The Glide virtual screening of retrieved drug-like *Juglans mandshurica* compounds against exportin-1 active site coordinate files in this study revealed L-epicatechin, epidihydrophaseic acid, KPT-185 (the standard compound), and eriodictyol (Figure 3) as respectively having molecular mechanics generalized born surface area (MMGBSA) dG binding free energy -41.42 kcal/mol, -40.77 kcal/mol, -34.9 kcal/mol, and -34.51 kcal/mol.

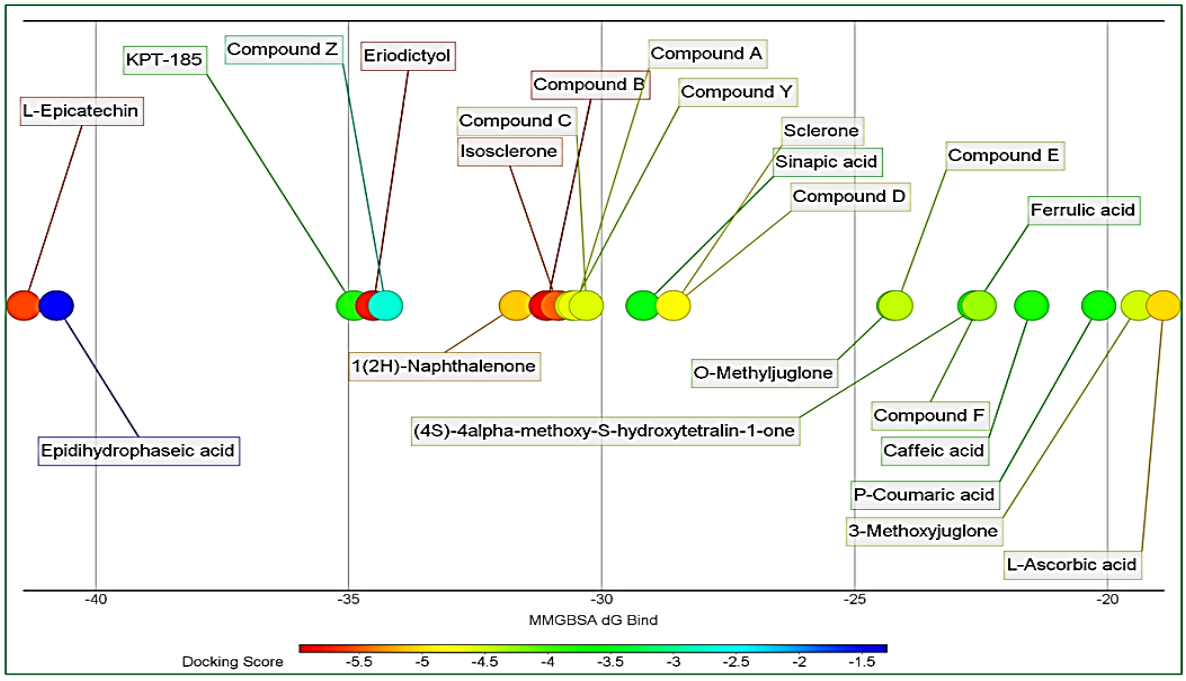

Figure 3: Graphical representation of docking scores and mmgbsa dg bind values of retrieved compounds following glide standard precision ligand docking

Quantum mechanics polarized ligand docking results: The quantum polarized ligand docking of the hit compounds against the exportin-1 active site coordinate files revealed L-epicatechin, epidihydrophaseic acid, KPT-185 (the standard compound), and eriodictyol as respectively having binding free energy -37.59 kcal/mol, -21.91 kcal/mol, -39.56 kcal/mol, and -40.74 kcal/mol as shown in Figure 4.

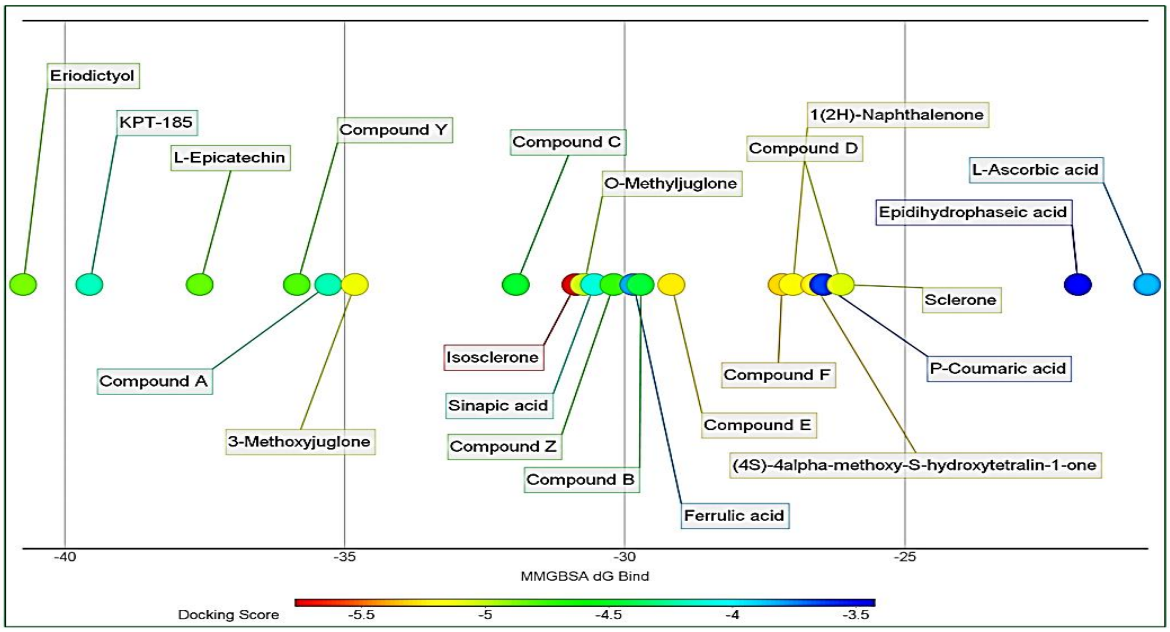

Figure 4: Graphical representation of docking scores and MMGBSA DG bind values of retrieved compounds following quantum polarized ligand docking

Validation of docking studying protocol through redocking of Exportin-1 Co-Crystal (KPT-185):

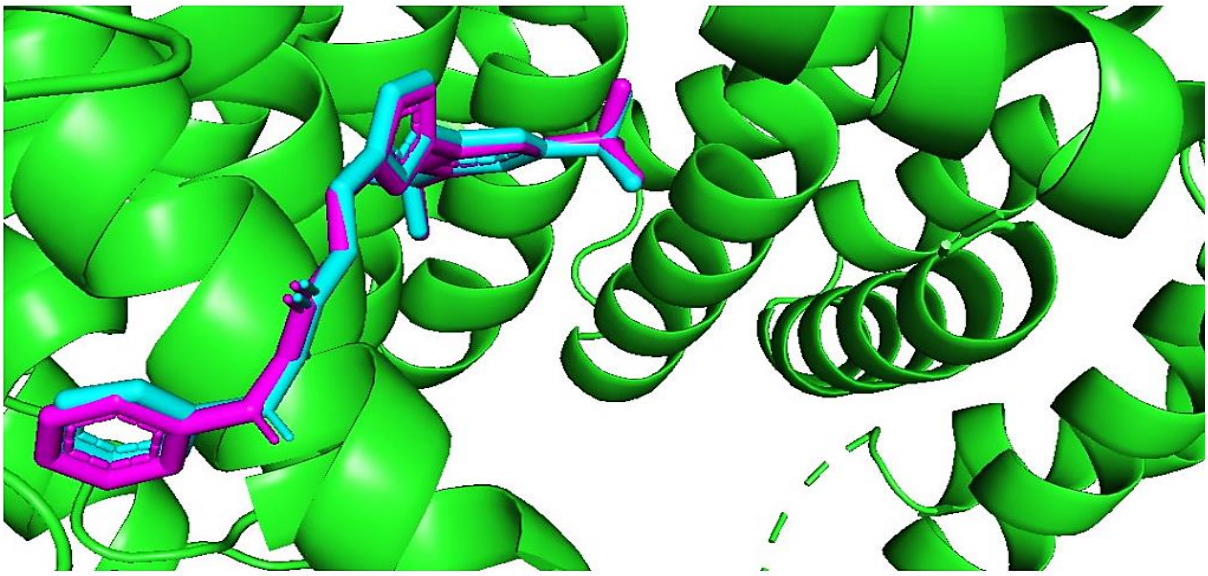

Figure 5: Superimposition of Co-Crystal ligand at the Exportin-1 active site following redocking

Table 4: Comparative compound docking scores using different algorithms

Ligand/Algorithm	PyRx (kcal/mol)	SwissDock (kcal/mol)	MVD (Re-rank Score) (kcal/mol)	Argus Lab (kcal/mol)	Glide MMGBSA (dG)
Eriodictyol	-6.7	-7.87	-89.6753	-9.27391	-40
KPT-185	-6.1	-7.23	-105.158	-7.53932	-39.56

Exportin-1 active residues iinteraction analysis: otable exportin-1 active residues forming conventional hydrogen bonding with both compounds include Asn 456 and Glu 459 (Figure 6A, 6B), while eriodictyol formed additional hydrophobic (Pi-sigma) and electrostatic (Pi-cation) bond interaction instead with Lys 455 residue (Figure 5B). The bond distance between eriodictyol and exportin-1 active site residues is 2.1199 Å – 3.0632 Å (Figure 5B), while the bond distance between KPT-185 and the target active site residues is in the range of 2.0808 Å – 4.7624 Å (Figure A).

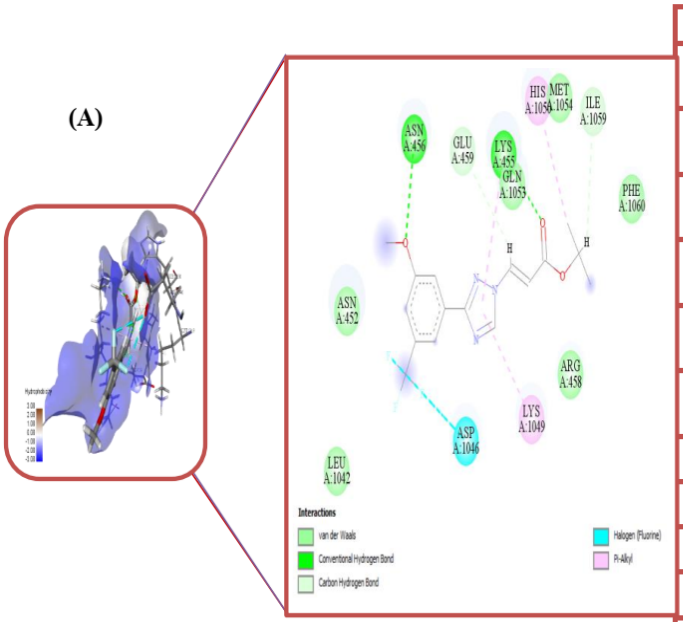

Name	Distance (Å)	Category	Types
A:LYS455:HZ1 - :UNK900:O2	2.85444	Hydrogen Bond	Conventional Hydrogen Bond
A:ASN456:HD22 - :UNK900:O1	2.08077	Hydrogen Bond	Conventional Hydrogen Bond
A:LYS455:HE2 - :UNK900:O2	3.09531	Hydrogen Bond	Carbon Hydrogen Bond
:UNK900:H7 - :UNK900:O2	2.43236	Hydrogen Bond	Carbon Hydrogen Bond
:UNK900:H8 - A:GLU459:OE2	2.9066	Hydrogen Bond	Carbon Hydrogen Bond
:UNK900:H10 - A:ILE1059:O	2.82517	Hydrogen Bond	Carbon Hydrogen Bond
A:ASP1046:OD1 - :UNK900:F1	3.0684	Halogen	Halogen (Fluorine)
A:ASP1046:OD1 - :UNK900:F3	3.13832	Halogen	Halogen (Fluorine)
A:HIS1050 - :UNK900:C16	3.50266	Hydrophobic	Pi-Alkyl
:UNK900 - A:LYS455	4.48826	Hydrophobic	Pi-Alkyl
:UNK900 - A:LYS1049	4.76235	Hydrophobic	Pi-Alkyl

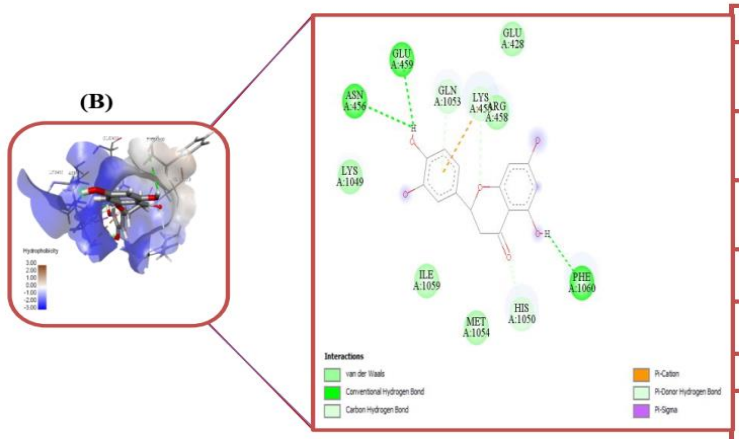

Name	Distance (Å)	Category	Types
:UNK900:H5 - A:PHE1060:O	3.06324	Hydrogen Bond	Conventional Hydrogen Bond
:UNK900:H12 - A:ASN456:OD1	2.96007	Hydrogen Bond	Conventional Hydrogen Bond
:UNK900:H12 - A:GLU459:OE2	2.11987	Hydrogen Bond	Conventional Hydrogen Bond
A:LYS455:HE2 - :UNK900:O2	2.5258	Hydrogen Bond	Carbon Hydrogen Bond
A:HIS1050:HE1 - :UNK900:O1	2.9139	Hydrogen Bond	Carbon Hydrogen Bond
A:LYS455:NZ - :UNK900	4.8202	Electrostatic	Pi-Cation
A:GLN1053:HE21 - :UNK900	2.40812	Hydrogen Bond	Pi-Donor Hydrogen Bond
A:LYS455:HD3 - :UNK900	2.92634	Hydrophobic	Pi-Sigma

Figure 6: Representation of ligand-target interaction. Figure shows **(A)** Interaction between KPT-185 and Exportin-1 **(B)** Interaction between Eriodictyol and Exportin-1

Comparative density functional theory properties showing chemical reactivity and stability of Eriodictyol and KPT-185

Table 5: Density functional theory properties estimations of Eriodictyol

Compound	HOMO Energy	LUMO Energy	Gap Energy	Average Ionization Energy	Electron Density	Electrostatic Potential
Eriodictyol	(A) -0.05	(B) - 0.05	0	(C) 193.335	0.001	(D) -49.3985
KPT-185	(E) -0.05	(F) - 0.05	0	(G) 196.049	0.001	(H) -36.4269

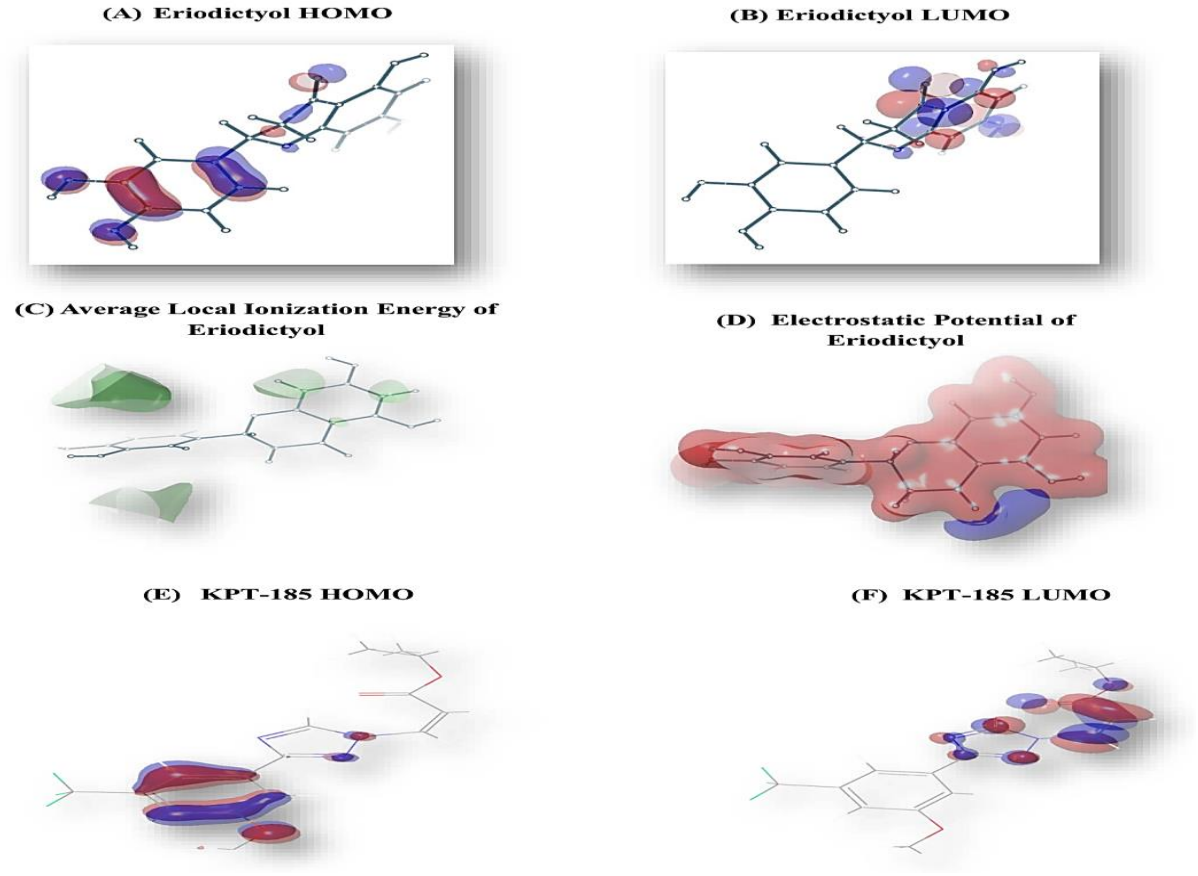

(G) Average Local Ionization Energy of KPT-185

(H) Electrostatic Potential of KPT-185

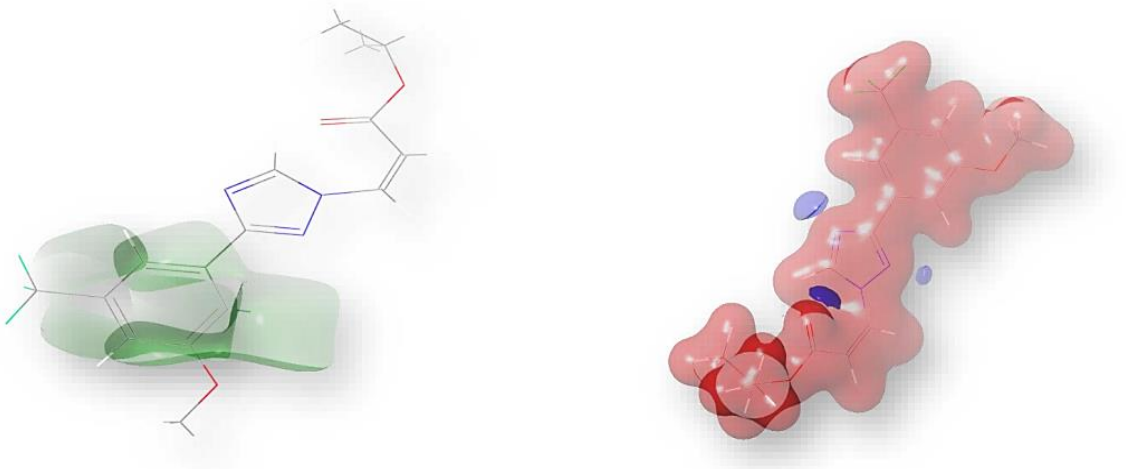

Figure 7: Density functional theory properties of Eriodictyol and KPT-185
*Blue Colour: Region of Concentrated Protons of Compound in Post Docking Pose and Energy State
*Red Colour: Region of Concentrated Electrons of Compound in Post Docking Pose and Energy State
*Green Colour: Region of Ionization and Reactivity of Compound and Energy State

Comparative pharmacokinetics and toxicity of compounds: Eriodictyol predictively exhibits non-inhibition of most of the commonly studied drug-metabolizing cytochrome P450 enzyme isoforms except CYP1A2 and CYP3A4 while KPT-185 displayed effective inhibitory property on the cytochrome P450 enzyme isoforms except CYP2D6 and CYP3A4 (Table 6). Also, eriodictyol displays positive predictive gastrointestinal permeability (shown in Table 6) similar to that of KPT-185 in this study but, unlike KPT-185, does not permeate the blood-brain barrier and displayed P-glycoprotein substrate properties. The lead-likeness screening of eriodictyol and KPT-185 through Brenk and PAINS filter analysis however revealed both as having the least tendency toward promiscuity in *in vitro* high throughput screening for future pre-clinical and clinical evaluations against exportin-1 (Table 6).

Table 6: Pharmacokinetics and toxicity profile of Eriodictyol

Compound	**KPT-185**	**Eriodictyol**
GI absorption	High	High
BBB permeant	Yes	No
P-glycoprotein substrate	No	Yes
CYP1A2 inhibitor	Yes	Yes
CYP2C19 inhibitor	Yes	No
CYP2C9 inhibitor	Yes	No
CYP2D6 inhibitor	No	No
CYP3A4 inhibitor	No	Yes
HepG2 Cytotoxicity	No	No
AMES	No	No
MMP	No	No
Brenk alert	1 (Michael acceptor)	0
PAINS alert	0	0

Drug-likeness and lead-likeness scores of compounds: Eriodictyol and KPT-185 have synthetic accessibility scores of 3.15 and 3.29 (Table 7) respectively on a scale of 1 (easy to synthesize) to 10 (very difficult to synthesize), the Abbot bioavailability score of both eriodictyol is 0.55 (Table 7) in similarity to that of KPT-185, while both compounds possess properties with non-violation of basic rules of conventional drug-likeness model including Lipinski's, Ghose's, Veber's, Egan's, and Muegge's as shown in Table 7. The lead-likeness profile of KPT-185 (Table 7) is however limited by its molecular weight greater than 350 while eriodictyol displays positive lead-likeness properties.

Table 7: Drug-likeness, lead-likeness, and synthetic accessibility score of Eriodictyol

Compound	KPT-185	Eriodictyol
Bioavailability Score	0.55	0.55
Lipinski's Violation	No	No
Ghose's violation	No	No
Veber's violation	No	No
Egan's violation	No	No
Synthetic accessibility score	3.29	3.15
Lead-likeness	No (1 violation) (MW > 350)	Yes

Discussion

The total of 133 compounds reported by some studies (Guo *et al*., 2015; Luo *et al*., 2017; Jahaban-Esfahlan *et al*., 2019) were retrieved in this study while a total of 22 (Table 1) with predictably non-toxic and drug-like compounds were recovered following the pre-filtering workflow on Osiris property explorer. Compound A-F, Y, Z were the identified but non-designated compounds from *Juglans mandshurica* with currently no structural information in the PubChem database while the first-generation SINE compound KPT-185 (PubChem CID: 53495165) was evaluated as the standard compound.

Complex balance exists between the molecular weight and other descriptors defining the oral bioavailability and bioactivity of compounds. Increased molecular weight positively associates with high bioactivity at the target active site but tends toward less bioavailability due to its reduced permeability potential (Veber *et al*., 2002; Ratomir *et al*., 2016). Hence the general consensus for predictably bioavailable and drug-like compounds have been modelled on the range of 160 ≤ molecular weight 500 (Lipinski *et al*., 2001; Ghose *et al*., 1999) which covers the molecular weight range (Table 2) of the 22 retrieved compounds in this study.

The water-octanol partition coefficient (ClogP), a well-recognized metric point value of a compound lipophilicity with defining impact on its bioavailability, of the retrieved compounds in this study falls within the range of -3.1715 to 2.4646. Furthermore, other physicochemical properties of the compounds (Table 2), including the number of hydrogen bond acceptors and donors as well as rotatable bond counts and total polar surface area obey the Veber *et al*. (2002) and Muegge *et al*. (2001) drug-like model rules.

The drug-likeness score (QED), quantifying the overall contribution of physicochemical and toxicity properties, is a useful metric for a compound potential as drug candidate. The prefiltered 22 compounds showed predictive toxicity level of none (no risk) to low (low risk) (Table 3) for tumorigenicity, mutagenicity, teratogenicity and irritant properties with quantitative estimate of drug-likeness (drug-likeness score) range of -1.3232 to 1.9964 in this study. Although the positive drug-likeness scores help qualifies the compounds as containing predominantly fragments frequently present in current commercially available drugs; this, however, may sometimes be representative of few physicochemical descriptors and therefore contributes only partially toward drug-like potential of the compounds (López-López *et al*., 2019). The complexity score of a compound is a defining feature on its solubility, permeability, oral bioavailability, promiscuity, as well as, in consequence, its clinical efficacy. It accounts for its number of aromatic rings, fraction of sp^3 hybridized carbons (Fsp^3), and negatively correlates with the compound developability and safety profile (Lagorce *et al*., 2017). The molecular complexity score of the 22 retrieved compounds in this study is in the range of 0.50742 to 1.0424 on a scale of 0.1 – 1.5. Also, the ligand conformational flexibility score is a measure of diverse assumable shapes based on molecular complexity score, dihedral bond angle changes and geometry weighting factors, which thereby plays pivotal role on its binding affinity and target specificity (Arteca, 1993; Forrey *et al*., 2012). The molecular flexibility score (Figure 2) of the 22 retrieved compounds in this study is in the range of 0.08271 to 0.50646 on a scale of 0.0 (flexible) to 1.0 (completely rigid), which thereby reveals the 22 retrieved compounds as having moderate to high conformational flexibility.

The recent development of exportin-1 inhibitors has excluded the overexpressed protein from orphan receptor category in NSCLC therapeutic strategies, but limitations abound around the efficacy, potency, and safety of these drug entities. This, therefore, predates the need for discovery and development of better new drug-like molecule entity. The Glide virtual screening of retrieved drug-like *Juglans mandshurica* compounds against exportin-1 structure coordinate files in this study revealed L-epicatechin, epidihydrophaseic acid as having relatively higher binding free energy and eriodictyol having binding free energy at very close range (-34.51kcal/mol - 34.9kcal/mol) when compared to -34.9kcal/mol of the standard compound (KPT-185) as the benchmark score. This suggests the potential relatively higher affinity, and in consequence, efficacy of these hits at the exportin-1 active site. The atomic valence electrons are always in motion around the molecule (Duan *et al*., 2020). Therefore, considering the partial charges being contributed by each compound fragments to binding

affinity at the target binding site has proven to be effective means toward accurate binding free energy calculations. This is done by applying the plausible target residue-ligand charge polarization in the calculation of the ligand binding energy at the best possible conformation. This returned eriodictyol (Figure 4) as only having the relatively higher binding free energy than KPT-185 in this study, thereby revealing it as the putative lead drug-like exportin-1 inhibitor. Furthermore, the superimposition of conformational binding poses of the redocked KPT-185 at the exportin-1 active site (Figure 5) in this study shows positive validity of the ligand docking procedure while the results from other docking algorithms (Table 4) further confirmed this study Glide docking scores.

The binding energy and, in consequence, efficacy of a drug entity at the target site is a function of nature and number of its interactions with the target residues. Examining the relative bonding interaction of the compounds and their prospective contribution to binding energy formation reveals eriodictyol formed relatively higher number of hydrogen interaction and fewer number of hydrophobic interactions at shorter bond distance to the target residues (2.1199 Å – 3.0632 Å of eriodictyol versus 2.0808 Å – 4.7624 Å of KPT-185) than that of KPT-185 (Figure 6). Notable exportin-1 active residue showing conventional hydrogen bonding interaction with both compounds include Asn 456 and Glu 459 while eriodictyol formed carbon-hydrogen bond with additional hydrophobic (Pi-sigma) and electrostatic (Pi-cation) bond interaction instead with Lys 455. The quantity and nature of hydrogen bonding interaction has been widely observed to have positive directional consequence for activity of drug entities (Patrick, 2013) and may have contributed to the relatively higher binding energy of eriodictyol.

The characteristic quantum property of a molecular entity is the bedrock of its degree of chemical reactivity and stability (Braga *et al*., 2016). Estimating therefore the pivotal gap energy between the electron-donating site (HOMO) and the site of less resistance to electrophilicity in the water solvation model of eriodictyol in this study (Table 5) revealed, through Becke's three-parameter Lee-Yang-Parr correlation method, an equal value of its lowest excitation energies with that of KPT-185. However, it shows lower electrostatic potential energy relative to KPT-185; a property defined by its degree of electron density cloud as shown in Figure 7D. This suggests relatively higher stability, with positive bearing toward ligand-receptor interaction, of eriodictyol than KPT-185 at the exportin-1 active site. Better pharmacokinetic profile of a drug molecule positively associates with its good potency, biostability, and safety profile. Eriodictyol, in this study, displays non-inhibition of most of the commonly studied drug-metabolizing cytochrome P450 enzyme isoforms (Table 5), a property that may plausibly contribute toward adjusting dose-bioavailability balance of the drug molecule en route the site of action. Although eriodictyol is notably a potential inhibitor of Cytochrome P450 3A4 (an enzyme responsible for hepatic degradation of most drug compounds) in this study (Table 5), there is need to establish the comparative percentage probability at which both compounds are liable to metabolic action of this enzyme in order to estimate the relative stability indices of the compounds as well as predict their relative potential toward inducing drug-drug interaction en route to the action site. This is because maintaining pivotal balance between metabolic stability and potency of a drug molecule, in respect to avoidance of toxic metabolite production or reduced efficacy, is a vital feature of effective drug discovery and development (Daina *et al*., 2017).

The positive predictive gastrointestinal permeability of eriodictyol in this study (Table 5) may well associate with its positive calculated log P value (Table 2) and thus shows its substantial lipophilicity potential as well as enhances its positive biological activity spectrum and selectivity potential.

Eriodictyol, unlike KPT-185, does not permeate the blood-brain barrier in this study (Table 5) but predictively a P-glycoprotein substrate. Both properties help in defining the possible biodistribution model of the compounds and while the former revealed the less possibility of eriodictyol, unlike KPT-185 (reported in some studies (Etchin *et al*., 2013; Azizian and Li, 2020), inducing any unintended central nervous system effect in the course of NSCLC therapy, the latter may help contribute to relative bioavailability and safety of the compound; although there is still a need to determine the relative percentage at which this occur en route to the target site.

The Brenk and PAINS filter (in accordance with various parameters as stated by Brenk *et al*., 2008) of both eriodictyol and KPT-185 in this study (Table 5) shows both as having least tendency of promiscuity in high throughput screening, thereby excluding the possibility of any substructure with non-selective bioactive response but reveal KPT-185, unlike eriodictyol, as having putatively toxic, chemically reactive Michael acceptor substructure that may have contributed to its associated side effects *in vivo*. This lends more credence to the potentially high safety and tolerability profile of eriodictyol as a putative exportin-1 inhibitor when compared to currently developed SINE compounds in the quest to develop better effective drug entity for NSCLC cure. The synthetic accessibility score of eriodictyol in this study (Table 6) also shows that it contains, in comparison to KPT-185, relatively higher frequent chemical moieties favourable for synthesis and low unfavourable rare moieties on a scale of 1 (easy to synthesized) to 10 (very difficult to synthesized) thereby presenting it as easy to synthesize for further preclinical and clinical evaluation. Drug-likeness and bioavailability are interdependent in determining the lead-likeness of a drug-like molecular entity (Teagle *et al*., 1999; Martin, 2005). The Abbot Bioavailability score of both eriodictyol and KPT-185 in this study reveal both

as highly Caco-2 cell permeable while the compounds obey all modelled rules of drug-likeness (Table 7). Eriodictyol also displays positive lead-likeness properties, unlike KPT-185, which is limited by molecular weight greater than 350, thereby revealing eriodictyol as a modifiable drug-like entity for possible lipophilicity enhancement (Table 7) and, in consequence, potency optimization.

Conclusion

The increasing global prevalence, associating morbidities, and the mortality rate of non-small cell lung cancer has rendered significant the discovery of new drug entity with better potency, pharmacokinetic, and safety profile in its chemotherapeutic approach. This study has revealed eriodictyol as a putative exportin-1 inhibitor with potentially better pharmaco-dynamo-kinetic properties than the current SINE compounds under pre-clinical and clinical studies. There is a need therefore to further evaluate eriodictyol as a candidate exportin-1 inhibitor in both pre-clinical and progressively in clinical studies involving lung cancer therapy.

Author Contributions

Conceived and conceptualized: T.O.A.; study design: T.O.A., F.A.S., A.N.; methodology: T.O.A., F.A.S., A.N.; resources: T.O.A., F.A.S., A.N., M.A.A., C.E.O., T.E.A., U.O.O., A.P.O., S.O.A., I.Y.F., I.A.O., W.O.J., O.O.A., K.O.A.; writing—original draft preparation: T.O.A.; writing—critical review, revised version, and re-editing: T.O.A., K.O.A., F.A.S., W.O.J., C.E.O., T.E.A., U.O.O., I.A.O, A.P.O., S.O.A., I.Y.F., O.O.A., K.O.A.; project administration: T.O.A. and F.A.S.; principal investigator: T.O.A. All authors have read and agreed to the published version of the manuscript.

Conflicts of Interest

The authors declare no conflict of interest

.

References

Arteca GA: Global measure of molecular flexibility and shape fluctuations about conformational minima. J Comput Chem 14(6): 718-727 (CCC 0192-8651/93/060718-10). 1993.

Braga EJ, Corpe BT, Marinho MM, Marinho ES: Molecular electrostatic potential surface, HOMO–LUMO, and computational analysis of synthetic drug rilpivirine. Int J Sci Eng Res 7(7): 2229-5518. 2016.

Brenk R, Schipani A, James D, Krasowski A, Gilbert IH, Frearson J, Wyatt GP: Lessons learnt from assembling screening libraries for drug discovery for neglected diseases. Chem Med Chem 3: 435–444 (Doi: 10.1002/cmdc.200700139). 2008.

Daina A, Michielin O, Zoete V: SwissADME: A free web tool to evaluate pharmacokinetics, drug-likeness and medicinal chemistry friendliness of small molecules. Sci Rep 7: 42717 (doi: 10.1038/srep42717). 2017.

Duan G, Ji C, Zhang JZH: Developing an effective polarizable bond method for small molecules with application to optimized docking. RSC Adv 10: 15530-15540 (Doi: 10.1039?DORA01483D). 2020.

Etchin J, Sun Q, Kentsis A, Farmer A, Zhang ZC, Sanda T, Mansour MR, Barcelo C, McCauley D, Kauffman M, Shacham S, Christie AL, Kung AL, Rodig SJ, Chook YM, Look AT: Anti-leukaemic activity of nuclear export inhibitors that spare normal hematopoietic cells. Leukemia 27: 66–74 (Doi: 10.1038/leu.2012.219). 2013.

Forrey C, Douglas JF, Gilson MK: The fundamental role of flexibility on the strength of molecular binding. Soft Matter 8(23): 6385-6392 (doi: 10.1039/C2SM25160D). 2012.

Ghose AK, Viswanadhan VN, Wendoloski JJ: A knowledge-based approach in designing combinatorial or medicinal chemistry libraries for drug discovery. 1. A qualitative and quantitative characterization of known drug databases. J Comb Chem; 1: 55–68. 1999.

Lagorce D, Douguet D, Miteva MA, Villoutreix BO: Computational analysis of calculated physicochemical and admet properties of protein-protein interaction inhibitors. Sci Rep 7: 46277 (doi: 10.1038/srep46277). 2017.

Lipinski CA, Lombardo F, Dominy BW, Feeney PJ: Experimental and computational approaches to estimate solubility and permeability in drug discovery and development settings. Adv Drug Deliv Rev 46(1-3): 3-26. 2001.

López-López E., Naveja JJ, Medina-Franco JL: DataWarrior: An evaluation of the open-source drug discovery tool. Expert Opin Drug Discov 14(4): 335-341 (doi: 10.1080/17460441.2019.1581170). 2019.

Muegge I, Heald SL, Brittelli D: Simple selection criteria for drug-like chemical matter. J Med Chem 44(12): 1841-1846. 2001.

Patrick GL: Drugs and Drug Targets: An Overview. *An Introduction to Medicinal Chemistry* pp: 6-7 (Oxford University Press). 2013.

Veber DF, Johnson SR, Cheng HY, Smith BR, Ward KW, Kopple KD: Molecular properties that influence the oral bioavailability of drug candidates. J Med Chem 45(12): 2615-2623. 2002.

Wang AY, Liu H: The past, present, and future of CRM1/XPO1 inhibitors. Stem Cell Investig 6: 6. 2019.